Experimental and theoretical study of the solubility of carbon dioxide in aqueous blends of piperazine and N-methyldiethanolamine

Derks, P. W. J.; Hogendoorn, J. A.; Versteeg, G. F.

Published in:
Journal of chemical thermodynamics

DOI:
10.1016/j.jct.2009.07.025

J. Chem. Thermodynamics 42 (2010) 151–163

Contents lists available at ScienceDirect

J. Chem. Thermodynamics

journal homepage: www.elsevier.com/locate/jct

Experimental and theoretical study of the solubility of carbon dioxide in aqueous blends of piperazine and N-methyldiethanolamine

P.W.J. Derks [a,b,*], J.A. Hogendoorn [c], G.F. Versteeg [d]

[a] Procede Gas Treating BV, P.O. Box 328, 7500 AH Enschede, The Netherlands
[b] University of Twente, Faculty of Science and Technology, P.O. Box 217, 7500 AE Enschede, The Netherlands
[c] University of Twente, Faculty of Science and Technology, Thermo-Chemical Conversion of Biomass Group, P.O. Box 217, 7500 AE Enschede, The Netherlands
[d] University of Groningen, Stratingh Institute for Chemistry and Technology, Chair of Process Technology, 9747 AG Groningen, The Netherlands

ARTICLE INFO

Article history:
Received 2 December 2008
Received in revised form 27 July 2009
Accepted 31 July 2009
Available online 11 August 2009

Keywords:
Piperazine
N-methyldiethanolamine
Carbon dioxide
Equation of state
Equilibrium
Solubility

ABSTRACT

In the present study, new experimental equilibrium data are reported on the solubility of carbon dioxide into aqueous solutions of N-methyldiethanolamine (MDEA) and piperazine (PZ) over a wide range of conditions. These data not only include CO_2 solubilities and their corresponding partial pressures, pH, and conductivities, but also a limited number of liquid speciation data obtained using NMR spectroscopy. The present data, and other data reported in the literature, were correlated with the Electrolyte Equation of State, as originally introduced by Fürst and Renon. The final model was able to describe the thermodynamics of the quaternary CO_2–PZ–MDEA–H_2O reasonably well over a wide range of experimental conditions.

1. Introduction

The technology of adding small amounts of an accelerator to an aqueous solution of a tertiary (alkanol)amine has found widespread application in the selective or bulk removal of carbon dioxide from process gas streams. The principle behind the use of these solvents is based on the relatively high rate of reaction of carbon dioxide with the accelerator, usually a primary or secondary amine, and the low reaction enthalpy of CO_2 with the tertiary amine. This leads to higher absorption rates in the absorber section, while maintaining a low energy penalty due to regeneration of the solvent in the desorber column. One commonly used solvent nowadays is a piperazine (PZ) activated aqueous solution of N-methyldiethanolamine (MDEA). Indispensable for a good understanding of the behavior of these amine solutions in the absorption–desorption process is a detailed knowledge on the thermodynamics of the solvent. On one hand, the CO_2 equilibrium partial pressure over a loaded amine solution determines the operating window in absorber and stripper, while, on the other hand, a thermodynamic model can provide information on the speciation of the solvent, which – among other things – determines (local) driving forces, reactions rates and hence rates of absorption. Although a piperazine activated aqueous MDEA solution is a commonly used solvent these days, only few studies on the thermodynamics of this system have been reported in the literature.

Xu *et al.* [1] investigated the effect of the addition of piperazine on the equilibrium partial pressure and liquid loading of carbon dioxide in aqueous MDEA solutions. They reported CO_2 liquid loadings and corresponding partial pressures over solutions containing 4.28 kmol · m^{-3} MDEA and PZ concentrations up to 0.515 kmol · m^{-3}. Liu *et al.* [2], from the same research group as Xu *et al.* [1], determined experimental CO_2 solubilities over a wide range of conditions. They varied both the piperazine and the MDEA concentrations, as well as the temperature in their experiments. Moreover, they described their data using two modelling approaches: a thermodynamic model that incorporates an extended Debye–Hückel expression, and a more simple Kent–Eisenberg approach. Neither of the models derived, however, included any of the carbamated piperazine species [$PZCOO^-$, $^+HPZCOO^-$, and $PZ(COO^-)_2$].

Bishnoi and Rochelle [3] reported experimental carbon dioxide solubilities in a 4.0 kmol · m^{-3} MDEA aqueous solution activated with 0.6 kmol · m^{-3} PZ at temperatures of (313 and 343) K and partial pressures up to approximately 7.5 kPa. In addition to the solubility data, they also measured the speciation of the liquid for one MDEA–PZ solution loaded with CO_2 using NMR spectroscopy. They applied the Electrolyte NRTL model to describe their solubility data

* Corresponding author. Address: Procede Gas Treating BV, P.O. Box 328, 7500 AH Enschede, The Netherlands. Tel.: +31 537112513; fax: +31 537112599.
E-mail address: peterderks@procede.nl (P.W.J. Derks).

0021-9614/$ - see front matter © 2009 Elsevier Ltd. All rights reserved.
doi:10.1016/j.jct.2009.07.025

and NMR (speciation) data. The obtained model was able to predict the experimental data of Xu *et al.* [1] and Liu *et al.* [2] reasonably well.

Pérez-Salado Kamps *et al.* [4] studied the experimental solubility of CO_2 in aqueous solutions of 2 mol · kg^{-1} MDEA and 2 mol · kg^{-1} PZ at a temperature of 353 K, and at total pressures ranging from (0.18 to 6.4) MPa. Also, a thermodynamic model, based on Pitzer's equation, was developed and model predictions were compared to the experimental data available at that time. It was found that the model was not able to accurately describe the experimental data taken at CO_2 partial pressures below 100 kPa. It should be noted, however, that no additional (fit) parameters were present in the model to account for the interactions between PZ- and MDEA-species, such as, *e.g.* between $PZCOO^-$ and $MDEAH^+$.

Si Ali and Aroua [5] studied the effect of piperazine on the equilibrium CO_2 liquid loading in an aqueous MDEA solution experimentally. Hereto, they determined the CO_2 loading – at constant temperature and CO_2 partial pressure – in aqueous MDEA solutions at concentrations of (2.0, 1.98, 1.90, and 1.80) kmol · m^{-3} with respectively (0, 0.01, 0.05, and 0.1) kmol · m^{-3} PZ (hence keeping the total "amine-group" concentration constant in all experiments). They concluded that the addition of PZ increased the solubility of CO_2 in the low partial pressure region when compared to 'pure' MDEA solutions.

This study will focus on the thermodynamics of the equilibrium solubility of CO_2 in aqueous solutions containing both PZ and MDEA. Firstly, new experimental CO_2 solubility data will be presented to extend the existing experimental database on this system. These new data not only include equilibrium pressure data, but also corresponding information on the liquid pH and conductivity of the loaded solvent. Also, a limited number of experimental speciation data will be presented that have been obtained using NMR spectroscopy. Secondly, in this work a thermodynamic model is developed to correlate the experimental data currently available in the literature. The thermodynamic model used in this work is based on the Electrolyte Equation of State (EoS), as originally introduced by Fürst and Renon [6]. This approach has been used to successfully describe CO_2 and/or H_2S solubilities in aqueous systems containing MDEA, MEA or DEA [7–10], and in Derks *et al.* [11], it was also proven to be suitable for describing the solubility of carbon dioxide in aqueous piperazine solutions.

2. Experimental

As mentioned in the previous section, this work includes experimental VLE data, which provide information on the solubility and corresponding partial pressure of CO_2 in aqueous MDEA/PZ solutions, as well as a limited number of liquid speciation data obtained with NMR spectroscopy for these solutions. The experimental methods and procedures that have been used to obtain these data will be described in this section.

2.1. (Vapor + liquid)-equilibrium experiments

The experimental setup used in this work was essentially the same as the 'continuous setup' used in a previous study [11], and will therefore not be described in detail. However, some modifications were made to make the setup suitable for the determination of pH and conductivity for the experiments in the present work.

- Firstly, the reactor was connected to a calibrated gas vessel, which was equipped with both a digital pressure transducer and a thermocouple. The presence of the gas vessel made it possible to supply a certain amount of pure CO_2 to the solution in the reactor.
- Secondly, a sampling loop (total volume about 200 mL) was attached to the reactor for measuring the liquid's pH and conductivity during an experiment. In the sampling loop, a small liquid pump was installed and operated in such a way that the average residence time inside the loop was well below 60 s. Insulation was applied to the entire sampling loop to avoid heat loss, and, to be able to verify this, also the 'returning' liquid temperature was measured with a thermocouple. The actual measuring electrodes were placed straight-up inside a small glass vessel within the loop. The liquid's pH was determined with a Mettler DG 111-SC pH electrode, which was calibrated using standard buffer solutions with known pH. A Radiometer CDC 104 (nominal cell constant 1.0 cm^{-1}) type electrode connected to an analogous conductivity meter type CDM 2d was used to measure the conductivity of the solution.

A schematic drawing of the setup is shown in figure 1. For a detailed picture of the setup, the reader is referred to Derks *et al.* [11].

In a typical experiment, known amounts of both piperazine (99%, Aldrich) and MDEA (99%, Aldrich) were dissolved in water and transferred to the reactor. Here, the solution was degassed by applying vacuum for a short while, and subsequently allowed to equilibrate at the desired temperature, after which the (vapor) pressure was recorded. Simultaneously, the gas supply vessel was filled with pure CO_2 and the initial pressure in this vessel was noted. Now, the stirrer in the reactor was switched on and a desired amount of carbon dioxide was fed from the gas supply vessel to the reactor. Then, the gas supply vessel was closed and the contents of the reactor was allowed to reach equilibrium, which was achieved, usually within about 30 min, when the reactor temperature and pressure as well as the pH and conductivity measured in the sampling loop remained constant. The total amount of carbon dioxide fed to the reactor was then determined by the initial and end pressure in the gas supply vessel, according to

$$n_{CO_2} = \frac{V^{GV}\Delta p^{GV}}{RT^{GV}}. \quad (1)$$

The use of the ideal gas law in equation (1) is allowed, as the maximum pressure in the gas supply vessel never exceeded 4 bar. The corresponding liquid loading at a certain CO_2 partial pressure is then determined by

$$\alpha_{CO_2} = \frac{1}{V^{R}_{liq}(c_{MDEA} + c_{PZ})} \cdot \left(n_{CO_2} - \frac{p^{R}_{CO_2} V^{R}_{gas}}{RT^{R}} \right). \quad (2)$$

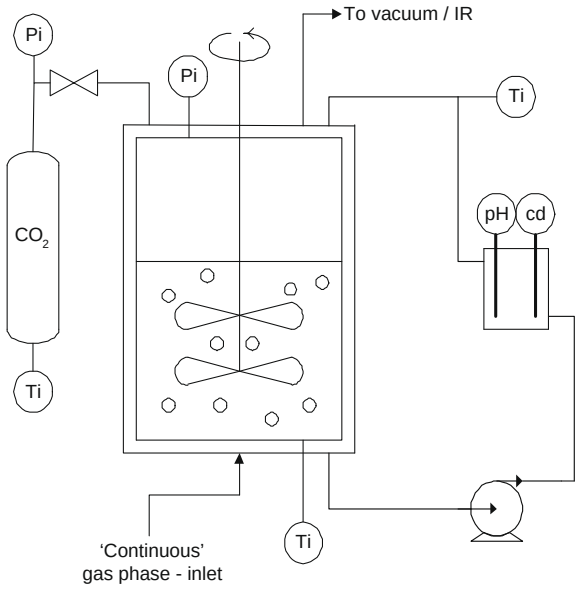

FIGURE 1. Schematic drawing of the reactor part in the experimental setup.

The method that was used to determine the corresponding partial pressure depended on whether the setup was operated in a batch-wise or continuous mode of operation during the experiment.

2.2. Procedure 'continuous experiments'

In experiments where the equilibrium partial pressure of CO_2 was expected to lie below about 10 kPa, the setup was operated in a continuous mode with respect to the gas phase. During these experiments, a gas flow consisting of N_2 and CO_2 was – after presaturation by an amine solution and water respectively – sent to the reactor, and the CO_2 concentration in the outgoing gas stream was measured using an IR analyzer, type UNOR 610. The composition of the inlet gas stream was adjustable and controlled by two calibrated mass flow controllers (MFCs). Now, upon attainment of equilibrium in the reactor, initially a small sweep stream of pure N_2 gas was passed through the reactor, and the CO_2 content of the outgoing gas stream was measured. The sweep stream was sufficiently small – and hence the gas phase residence time sufficiently large – to ensure that the outgoing gas concentration was at near-equilibrium. Next, the MFC controlling the carbon dioxide gas flow was set to such a value, that the composition of the inlet flow would match the measured outlet composition. This 'trial & error' procedure of adjusting the carbon dioxide MFC (and hence inlet composition) to the detected CO_2 content in the outlet, was repeated until the IR analyzer did give a stable signal. At this point, usually attained within about (20 to 30) min, the inlet gas composition (set by the MFCs) matched the outlet composition, which in turn determines the equilibrium composition of the gas in this experiment.

2.3. Procedure 'batch experiments'

In experiments where the equilibrium partial pressure of CO_2 exceeded 10 kPa, the reactor was operated batch-wise with respect to the gas phase. Now, the CO_2 partial pressure was directly calculated from the total equilibrium pressure in the reactor corrected for the lean solution vapor pressure. Hereby, it was implicitly assumed that the vapor pressure was not influenced by the amount of CO_2 present in the solution.

2.4. Validation

The experimental setup and procedures were validated by measuring the carbon dioxide solubility in an aqueous solution of 2.0 kmol · m^{-3} MDEA at 313 K, a system for which results are extensively reported in the literature. Results are listed in table 1 and compared to literature sources in figure 2.

Figure 2 shows that the new experimental data are well in line with solubility data reported in the literature and therefore the results obtained with the current experimental setup and using the experimental procedures can be considered to be reliable.

TABLE 1
CO_2 partial pressure p_{CO_2} as a function of loading α_{CO_2} in 2.0 kmol · m^{-3} aqueous MDEA at T = 313 K.

α_{CO_2}	p_{CO2}/kPa	Gas phase mode of operation
0.122	1.25	Continuous
0.213	3.24	Continuous
0.294	5.97	Continuous
0.361	8.5	Batch
0.382	9.2	Batch
0.478	15.4	Batch
0.610	30.0	Batch
0.627	32.4	Batch
0.807	93.6	Batch
0.810	91.6	Batch

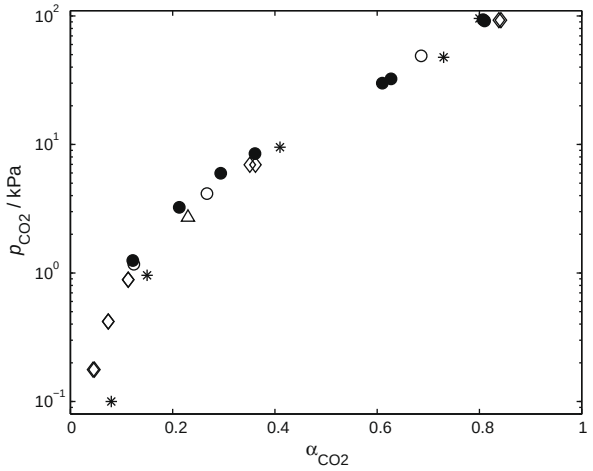

FIGURE 2. CO_2 partial pressure p_{CO_2} as a function of loading α_{CO_2} in 2.0 kmol · m^{-3} aqueous MDEA at T = 313 K: ●, this work; ◇ Austgen and Rochelle [12]; ○, Mac Gregor and Mather [13]; △, Huang and Ng [14]; ∗, Si Ali and Aroua [5].

2.5. NMR spectroscopy experiments

Carbon dioxide partial pressure data are generally the kind of equilibrium solubility data used in the regression of (thermodynamic) parameters present in acid gas equilibria modelling. However, the ability of a model to describe or predict equilibrium pressures, does not automatically imply that it can also correctly predict the liquid phase speciation – which in turn is a vital input in the rate-based rigorous modelling of both the absorption and desorption column. The model predicted speciation can, partly and indirectly, be validated with the use of experimental pH and conductivity data, if available, as these data provide information on the activity of the H_3O^+ (and the OH^-) ion and on the total ion concentration present in solution. Even more specific information on the liquid phase composition of a loaded (alkanol)amine solution can be obtained using NMR spectroscopy, as illustrated in the literature [3,15–17]. To obtain more information on the liquid phase speciation as a function of carbon dioxide loading also in this study the liquid phase composition of an aqueous 4.0 kmol · m^{-3} MDEA, 1.0 kmol · m^{-3} PZ has been determined using NMR measurements at 298.15 K. The experimental procedure regarding the NMR spectroscopy and required details are described below.

The amine solution was prepared by dissolving known amounts of piperazine (purity 99%, Aldrich) and MDEA (purity 99%, Aldrich) in water and deuterium oxide (purity 99%, Aldrich). The final solution contained about 10 volume% D_2O to ensure a good 'lock signal' in the NMR apparatus.

Subsequently, about 0.8 mL of the solution was injected with a syringe into a Wilmad 528-PV-7 NMR tube. The NMR tube was connected to a calibrated gas supply vessel equipped with a Heise 3710 pressure transducer. A desired amount of carbon dioxide (quality 4.0, Hoekloos) was added from the gas supply vessel to the NMR tube, and the resulting CO_2 loading was calculated from the pressure difference in the gas supply vessel, using equations (1) and (2). In the loading calculation, it was assumed that the amount of CO_2 present in the gas phase was negligible compared to the amount absorbed by the liquid. Next, the sample tubes were allowed to equilibrate in a softly shaken thermostatted bath for at least a week, after which the NMR spectra were taken.

The liquid phase composition was determined using ^{1}H, ^{13}C, H–H, and C–H NMR spectroscopy on a Bruker Avancell 600 MHz spectrometer, equipped with a TXI (^{1}H, H–H, and C–H experiments) or BBO (^{13}C experiments and C–H experiments) probe. The 2D data were used to identify the individual peaks in the ^{1}H and ^{13}C spectra, whereas the ^{1}H NMR results were used for a more quantitative analysis of the different reaction products. As it is not possible with the presently applied method to distinguish between a base and its conjugate acid (*e.g.* MDEA and $MDEAH^+$) or the ratio of the two, without an extensive calibration procedure (see, *e.g.* [17]), only the following three (piperazine) groups could be quantified:

- piperazine, protonated piperazine and diprotonated piperazine,
- piperazine monocarbamate, and its protonated counterpart,
- piperazine dicarbamate.

The ratio between total MDEA and total PZ was used as an internal reference to check the consistency of the measurements.

3. Electrolyte equation of state modelling

3.1. General

When carbon dioxide is dissolved in an aqueous solution containing piperazine and MDEA, several (equilibrium) reactions take place:

Water dissociation: $2H_2O \leftrightarrows OH^- + H_3O^+$
Bicarbonate formation: $2H_2O + CO_2 \leftrightarrows HCO_3^- + H_{3O}^+$
Carbonate formation: $HCO_3^- + H_2O \leftrightarrows CO_3^{2-} + H_3O^+$
Piperazine protonation: $H_2O + PZH^+ \leftrightarrows PZ + H_3O^+$
Piperazine diprotonation: $H_2O + PZH_2^{2+} \leftrightarrows PZH^+ + H_3O^+$
Piperazine mono-carbamate hydrolysis: $PZ + HCO_3^- \leftrightarrows H_2O + PZCOO^-$
Piperazine di-carbamate hydrolysis: $PZCOO^- + HCO_3^- \leftrightarrows H_2O + PZ(COO^-)_2$
Monocarbamate protonation: $H_2O + {}^+HPZCOO^- \leftrightarrows PZCOO^- + H_3O^+$
MDEA protonation: $H_2O + MDEAH^+ \leftrightarrows MDEA + H_3O^+$

These nine independent equilibria – in combination with the piperazine, MDEA, H_2O/hydrogen and CO_2 mass balances and the electroneutrality criterion – results in a system of 14 equations to be solved for the 14 species that are taken into account in the model. The non-ideality of the system is taken into account using the Electrolyte Equation of State – which will be (shortly) described in the next section. It should be noted that, in the model, the presence of the carbonate ion (CO_3^{2-}), the diprotonated PZ species (PZH_2^{2+}) and the H_3O^+-ion was neglected for similar reasons given in Derks *et al.* [11].

3.2. Model buildup

The thermodynamic model applied in this work is the Electrolyte Equation of State (EoS), as originally introduced by Fürst and Renon [6], in which the system's non-ideality is calculated from (the sum of) four different contributions to the (reduced) free Helmholtz energy of the system A^R (see equation (3)):

$$\left(\frac{A - A^{IG}}{RT}\right) = \left(\frac{A^R}{RT}\right) = \left(\frac{A^R}{RT}\right)_{RF} + \left(\frac{A^R}{RT}\right)_{SR1} + \left(\frac{A^R}{RT}\right)_{SR2} + \left(\frac{A^R}{RT}\right)_{LR}. \quad (3)$$

The first two terms in equation (3) describe the molecular interactions (repulsive forces, RF, and short range interactions, SR1) in the system. Interactions between molecular and ionic species as well as ion-ion interactions are included in the second short range term (SR2). The fourth contribution to the reduced Helmholtz energy stems from the long range ionic forces (LR). All governing equations describing these individual contributions are listed in detail in Derks *et al.* [11], and will therefore not be given here.

The total model, which will be used to describe the quaternary H_2O–CO_2–PZ–MDEA system, requires – besides various physical and/or thermodynamic constants – several sets of pure, binary, or ternary (fit) parameters which need to be determined on beforehand on the corresponding subsystems. A schematic overview of the model structure is given in figure 3.

In Derks *et al.* [11], the Electrolyte EoS model was used to successfully describe the CO_2 solubility in aqueous piperazine solutions. From figure 3, it can be concluded that many parameters necessary for the present, quaternary system, model, are also parts of the previously developed model for the ternary system PZ–CO_2–H_2O. For information on the (method of) determination and/or estimation of these sets of parameters (marked with § in figure 3) and their respective values, the reader is therefore referred to Derks *et al.* [11]. The parameters of the ternary subsystem PZ–CO_2–H_2O are used "as is" in the quaternary system. The second ternary subsystem MDEA–CO_2–H_2O has been more frequently studied. From the experimental literature data available, the required EoS parameters will be derived. This is discussed in the next section.

3.3. Thermodynamics of the ternary (MDEA + CO_2 + H_2O) system

Before the model can be used to describe the quaternary system, also the (reactive) ternary system with MDEA needs to be correlated according to the EoS approach, since the majority of the remaining, unknown, parameters in the total model (marked with # in figure 3) are a part of this second ternary system, consisting of MDEA, carbon dioxide, and water.

Initially, the various pure component and binary interaction parameters were determined in a similar manner as in the previous work for PZ–CO_2–H_2O: The polar parameters p_1, p_2, p_3 of MDEA were fitted to experimental pure vapor pressure data [18–20], while both freezing point depression data [21] and VLE data [22–24] were used to regress the interaction parameters in the (MDEA + water) system. The molecular interaction between MDEA and CO_2, however, was differently described compared to the interaction between piperazine and carbon dioxide. Whereas in the latter system, one single mixing parameter, k_{mix}, was used to

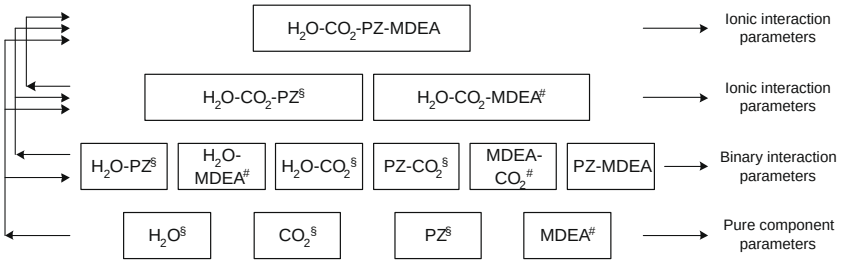

FIGURE 3. Schematic overview of the model structure.

describe this interaction, the Huron–Vidal mixing rule will be applied to model the MDEA - CO_2 molecular interaction, following the approach by Huttenhuis *et al.* [25]. They suggested to fit these binary, mixing parameters to the available (physical) N_2O solubility data in pure and aqueous MDEA, converted to physical CO_2 solubilities with the CO_2—N_2O analogy. The effect of applying the Huron–Vidal mixing rule ('New model') rather than the single parameter approach ('Old model') is illustrated in figure 4.

All resulting (pure and binary) fit parameters and the experimental data sources have been listed in table 2, along with the various physical and critical constants. All other, remaining parameters needed in the MDEA—CO_2—H_2O modelling, such as, *e.g.* the pure water parameters and the H_2O—CO_2 interaction parameters, can be found in Derks *et al.* [11].

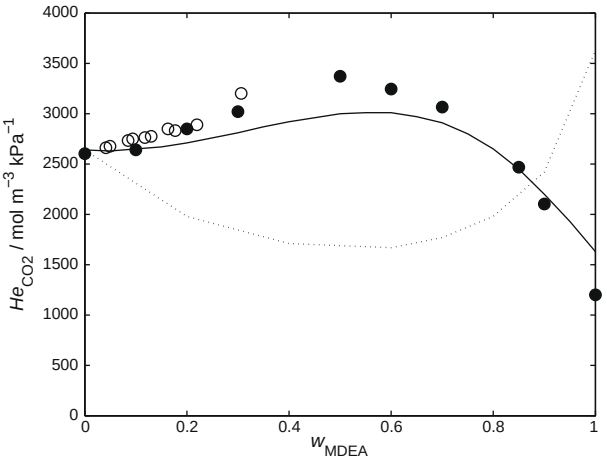

FIGURE 4. Henry coefficient of CO_2 He_{CO_2} in aqueous MDEA as a function of mass fraction MDEA w_{MDEA} at $T = 293$ K: 'solid circle', exp. data by Versteeg and Van Swaaij [26]; ○, exp. data by Kierzkowska-Pawlak and Zarzycki [27]; 'dotted line', 'Old model'; 'solid line', 'New model'.

TABLE 2
Parameters used in the modelling of the $(MDEA + CO_2 + H_2O)$ equilibrium.

Single component parameters		Binary systems	
MDEA		*H_2O–MDEA*	
p_C/bar	41.6	$\Delta g'_{12}/(\mathrm{kJ \cdot mol^{-1}})$	6.32
T_C/K	741.9	$\Delta g''_{12}/(\mathrm{J \cdot mol^{-1} \cdot K^{-1}})$	−43.2
Acentric factor	0.625	$\Delta g'_{21}/(\mathrm{kJ \cdot mol^{-1}})$	−10.08
Source	[20]	$\Delta g''_{21}/(\mathrm{J \cdot mol^{-1} \cdot K^{-1}})$	42.1
p_1	−0.0934	$\alpha_{12} = \alpha_{21}$	0.243
p_2	2.6802	Source	[21–24]
p_3	1.4847		
Source	[18–20]	*MDEA–CO_2*	
D_0[a]	−8.16	$\Delta g'_{12}/(\mathrm{kJ \cdot mol^{-1}})$	48.37
D_1	8989.3	$\Delta g''_{12}/(\mathrm{J \cdot mol^{-1} \cdot K^{-1}})$	−37.5
Source	[12]	$\Delta g'_{21}/(\mathrm{kJ \cdot mol^{-1}})$	−179
Molec. diameter/Å	4.50	$\Delta g''_{21}/(\mathrm{J \cdot mol^{-1} \cdot K^{-1}})$	83.2
Source[b]	[9]	$\alpha_{12} = \alpha_{21}$	−0.0002
	[10]	Source	[26–29]
$MDEAH^+$			
Ionic diameter/Å	4.50		
Source	[9,10]		

[a] The dielectric constant of MDEA is calculated from $D = D_0 + D_1/T$.
[b] All sources deduce the molecular diameter from the amine covolume.

The chemical equilibria considered in this subsystem are:

Water dissociation: $2H_2O \leftrightarrows OH^- + H_3O^+$
Bicarbonate formation: $2H_2O + CO_2 \leftrightarrows HCO_3^- + H_3O^+$
MDEA protonation: $H_2O + MDEAH^+ \leftrightarrows MDEA + H_3O^+$

All chemical equilibrium constants in this work are defined in the mole fraction scale with as reference state infinite dilution in water for all species except water, their temperature dependence is given by equation (4) and the corresponding coefficients $C_0 - C_2$ are listed in table 3

$$\ln K = C_0 + \frac{C_1}{T} + C_2 \ln T. \tag{4}$$

With respect to the implementation of the ternary MDEA system in the quaternary model, the following simplifications and assumptions have been made:

- The concentration of H_3O^+ in the solution is marginally small for typical operating conditions and can therefore be neglected, which is a generally accepted assumption considering the basic environment of aqueous alkanolamine – acid gas solutions.
- Also the presence of carbonate ions is neglected, based on the pH range of interest and the equilibrium constant for this reaction. The same simplification was adopted in previous equilibrium studies [9,10].
- Only interactions between cations and anions, and cations and molecular species were included in the model, all other ionic interactions were neglected – as in previous publications on the Electrolyte EoS modelling.
- The ionic interaction between $MDEAH^+$ and the hydroxide ion OH^- has been set to zero, as preliminary simulation runs showed that the influence of this parameter on the model outcome was negligibly small for typical operating conditions.

In the literature, many different experimental data series on the solubility of CO_2 in aqueous MDEA solutions have been reported, which could be used in the regression of the (four) remaining ionic interaction parameters for the ternary $(MDEA + CO_2 + H_2O)$ system (see table 5). In this work, the experimental database as suggested by Huttenhuis *et al.* [30] was used to fit the ionic interaction parameters. Huttenhuis *et al.* [30] critically reviewed the different available experimental data series, and they proposed a database which includes (internally and mutually consistent) solubility data over a wide range of temperature, MDEA concentration, and CO_2 loading. The objective function for minimization was the same as used throughout the entire study:

$$F = \min \sum_i \left| \frac{P_i^{\mathrm{exp}} - P_i^{\mathrm{mod}}}{P_i^{\mathrm{exp}}} \right|. \tag{5}$$

The values for the ionic interaction parameters resulting from the regression are listed in table 4, while the model correlation

TABLE 3
Coefficients for the chemical equilibrium constants used in the model.

	C_0	C_1	C_2	$K_{(T=313\ \mathrm{K})}$	T/°C	Source
Water dissociation	132.899	−13445.9	−22.4773	$9.3 \cdot 10^{-18}$	0 to 225	[31]
Bicarbonate formation	231.465	−12092.1	−36.7816	$9.0 \cdot 10^{-9}$	0 to 225	[31]
MDEA protonation	−83.490	−819.7	10.9756	$1.8 \cdot 10^{-12}$	5 to 95	[32]

TABLE 4
Ionic interaction parameters W_{kl} for the $(MDEA + CO_2 + H_2O)$ system.

$W_{kl}/(m^3 \cdot kmol^{-1})$	
$MDEAH^+ - H_2O$	0.112
$MDEAH^+$–MDEA	0.080
$MDEAH^+ - CO_2$	−0.105
$MDEAH^+ - HCO_3^-$	−0.127

TABLE 6
Legend to figures 6 and 7.

	Experiment	Model
MDEA	×	dotted line
$MDEAH^+$	+	Solid line
HCO_3^-	○	Solid line
CO_2	□	Dashed line

results are listed in table 5 and a graphical comparison between experimental and model predicted values is given in figure 5.

The results presented in table 5 and figure 5 show that the model is well able to describe experimental (carbon dioxide partial and total system) pressures as a function of the liquid loading for aqueous MDEA solutions. However, this ability alone is not a reliable hallmark for the quality of a thermodynamic model, as it does not tell whether the liquid phase speciation is correct. A thermodynamic model to be used in gas treating processes should not only be able to predict the CO_2 pressure *vs.* loading curve, but also the speciation of the liquid as a function of loading. This is because the speciation is required in the determination of the actual driving force for CO_2 absorption, and thus required for the rigorous mass transfer modelling used in the design and operation of industrial absorbers. The ability of the present model to predict the speciation of the ternary subsystem $(MDEA + CO_2 + H_2O)$ has been validated with a limited number of available experimental speciation data as reported by Poplsteinova Jakobsen *et al.* [17], who used NMR to determine the liquid composition of loaded aqueous MDEA solutions at $T = (20$ and $40)$ °C. A comparison between the model predictions and the experimental data is given in figures 6 and 7. From these speciation plots, it can be concluded that the model predicted speciation is well in line with the experimentally reported liquid composition. The model, however, does seem to overpredict the molecular CO_2 fraction in the liquid.

Additionally, the model has been tested using an experimentally determined physical property, namely the pH of a solution. Posey [33] measured the pH of an aqueous 50 wt.% MDEA solution as a function of carbon dioxide loading, and his results are compared to the model prediction in figure 8. Judging from this figure, it can be concluded that the model is able to predict the trend in pH fairly well, despite a seemingly constant offset between experimental value and model prediction.

3.4. Discussion

Based on the results obtained so far, the Electrolyte EoS model has proven to be suitable for describing both ternary (reactive) subsystems from which the $(MDEA + PZ + CO_2 + H_2O)$ system is "constructed". Derks *et al.* [11] already showed that the model was able to successfully describe CO_2 solubilities in aqueous piperazine solutions, and moreover, the model was found to predict experimentally observed pH and conductivity data well. It was shown in this work that also experimental (carbon dioxide partial) pressures over loaded MDEA solutions are correlated well by the Electrolyte EoS. Furthermore, the model predicted speciation was found to be well in line with experimental liquid composition data. Also, the model was found to predict the pH of a loaded MDEA solution fairly well. When considering the results concerning the speciation and pH, it should be kept in mind that the interaction parameters as now used in the model have been regressed using the available experimental pressure *vs.* loading data only.

When the two subsystems (second level from the top in figure 3) are combined to form the final quaternary model, basically two new (series of) interaction parameters are introduced:

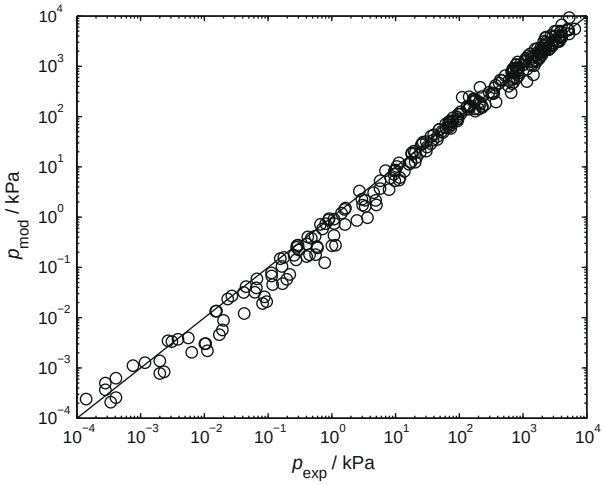

FIGURE 5. Parity plot on the $H_2O + CO_2 + MDEA$ system: Experiment *vs.* model. Data sources listed in table 5.

TABLE 5
Experimental $MDEA-H_2O-CO_2$ database and modelling results.

Reference	w_{MDEA}	T/K	α_{CO_2}	N	AAD/%
[34]	0.236	298	0.02 to 0.26	13	28.0
[12]	0.234	313	0.006 to 0.842	8	24.2
	0.490	313	0.00314 to 0.652	6	
[35]	0.192	313	0.79 to 1.23	9	17.8
	0.188	313, 333, 373, 413	0.18 to 1.25	32	
	0.321	313, 333, 373, 393, 413	0.11 to 1.16	40	
[36]	0.205	323, 348, 373	0.026 to 0.848	32	23.7
	0.500	323, 348, 373	0.0087 to 0.385	26	
[37]	0.320	313	0.85 to 1.24	5	30.6
	0.488	313, 353, 393	0.32 to 0.56	23	
[14]	0.23	313, 343, 373, 393	0.00334 to 1.34	29	33.2
	0.50	313, 343, 373, 393	0.00119 to 1.16	37	
[38]	0.23	313, 323	0.000591 to 0.1177	20	38.7
	0.50	313	0.000249 to 0.037	14	
Total				294	26.8

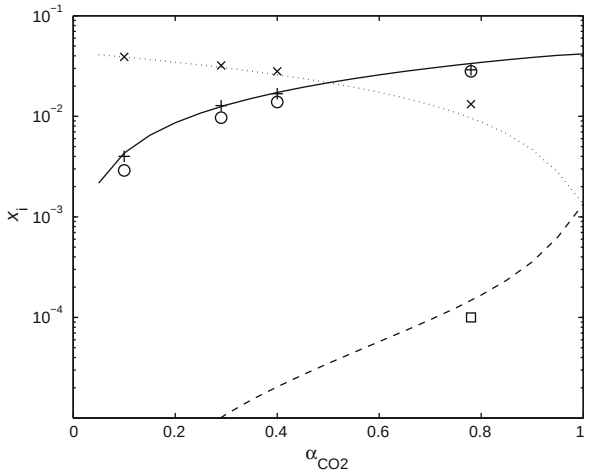

FIGURE 6. Liquid phase speciation x_i of an aqueous 23 wt.% MDEA solution at 20 °C as a function of CO_2 loading α_{CO2}. Symbols represent experimental data [17]. Lines represent model predictions. Full legend in table 6.

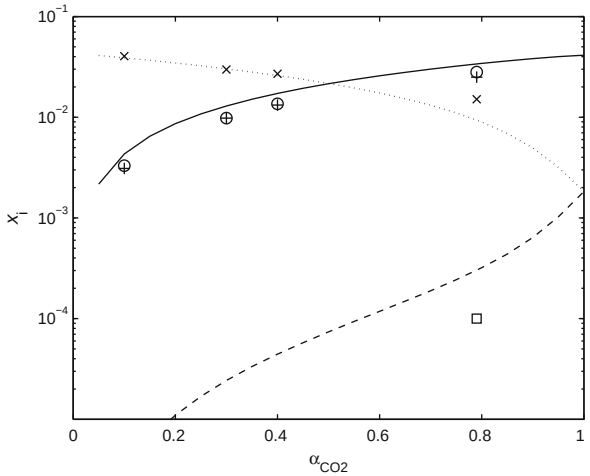

FIGURE 7. Liquid phase speciation x_i of an aqueous 23 wt.% MDEA solution at 40 ° C as a function of CO_2 loading α_{CO2}. Symbols represent experimental data [17]. Lines represent model predictions. Full legend in table 6.

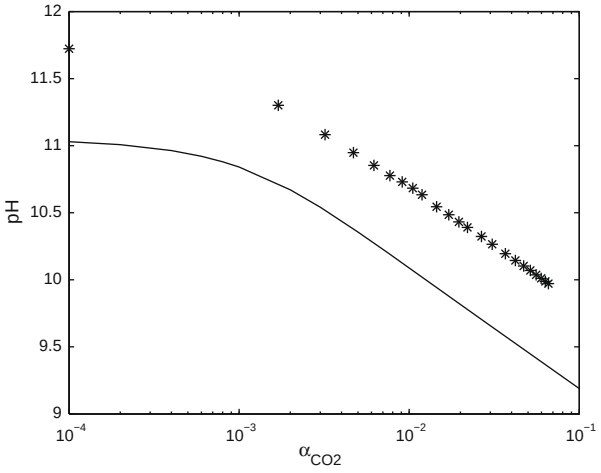

FIGURE 8. pH of an aqueous 50 wt.% MDEA solution at ≈ 22.5 °C as a function of CO_2 loading α_{CO_2}: ∗, experimental data by Posey [33]; 'solid line', model prediction.

TABLE 7
Experimental equilibrium data (CO_2 partial pressure p_{CO_2}, pH, and conductivity) in a 4.0 kmol · m^{-3} MDEA and 0.6 kmol · m^{-3} PZ solution at 313 K as a function of CO_2 loading α_{CO_2}.

α_{CO_2}	p_{CO_2}/kPa	pH	Cond./mS	α_{CO_2}	p_{CO_2}/kPa	pH	Cond./mS
0.062		9.99	1.70	0.327	12.6	9.07	6.50
0.123	0.72	9.61	2.90	0.339	12.8	9.02	6.90
0.126	0.90			0.426	25.3	8.88	8.20
0.178	2.07	9.38	4.00	0.498	39.0	8.78	9.50
0.189	2.70	9.35	3.80	0.504	39.0	8.76	9.40
0.232	4.36	9.24	5.30	0.568	58.4	8.65	10.45
0.250	5.24	9.21	4.70	0.578	60.4	8.65	10.5
0.283	7.00	9.14	6.20	0.621	78.5	8.65	11.0
0.284	7.33	9.14	5.60	0.632	80	8.58	11.1
0.310	9.38	9.09	6.25	0.638	89.7	8.62	11.3
0.312	8.65	9.07	6.90				

TABLE 8
Experimental equilibrium data (CO_2 partial pressure p_{CO_2}, pH, and conductivity) in a 2.8 kmol · m^{-3} MDEA and 0.7 kmol · m^{-3} PZ solution at 303 K as a function of CO_2 loading α_{CO_2}.

α_{CO_2}	p_{CO_2}/kPa	pH	Cond./mS	α_{CO_2}	p_{CO_2}/kPa	pH	Cond./mS
0.042		10.38	1.8	0.518	9.4	9.10	12.0
0.838		10.16	2.5	0.523	10.7	9.52	12.1
0.124		9.89	3.55	0.573	15.2	8.92	12.6
0.169		9.76	4.2	0.664	25.7	8.81	15.2
0.208	0.51	9.58	5.4	0.681	36.1	9.16	16.0
0.252	0.96	9.49	6.0	0.689	32.1	9.17	15.9
0.303	1.75	9.33	7.5	0.708	38.9	8.65	16.0
0.348	2.61	9.28	8.25	0.758	56.4	8.52	17.0
0.399	4.16	9.13	9.5	0.790	73.7	8.43	17.9
0.435	5.23	9.10	9.9	0.784	70.4	8.91	18.0
0.468	6.80	8.99	11.0	0.818	93.8	8.34	18.2
0.513	8.65	8.95	11.6	0.815	96.9	8.81	18.5
0.537	10.2	8.86	12.3	0.837	100.1	8.31	19.7

- Firstly, the (binary) molecular interaction between MDEA and piperazine needs to be identified.
- Secondly, five additional, mutual ionic interaction parameters are needed in the model. This group of parameters includes on one hand the interaction between $MDEAH^+$ and (neutral and negatively charged) piperazine-species, and, on the other hand, the interaction between PZH^+ and MDEA.

All these parameters are to be regressed over experimental solubility data in aqueous solutions containing both MDEA and piperazine. The results will be discussed later.

4. Experimental results

4.1. Equilibrium partial pressure results

All experimentally obtained solubilities of carbon dioxide in aqueous solutions of MDEA and PZ are listed in tables 7 to 11, along with the corresponding partial pressures, pH and conductivity data.[1] The experimental uncertainty in this work is estimated at 4% in loading. Depending on the type of experiment, the uncertainty in CO_2 partial pressure can amount to max. 10% in the continuous gas phase experiments and to 5% when the gas phase was batchwise operated, respectively. The experimentally determined pH data are estimated to be accurate within 0.1 pH point, while the uncertainty in the reported conductivities ranges from 0.05 mS (for conductivities ≦5 mS) up to 0.25 mS for higher conductivities.

[1] For the lowest CO_2 loading data points, the corresponding partial pressure has not been listed: At these loadings, the CO_2 partial pressure was (expected to be) too low to be accurately determined with the IR detector.

TABLE 9
Experimental equilibrium data (CO_2 partial pressure p_{CO_2}, pH and conductivity) in a 2.8 kmol · m^{-3} MDEA and 0.7 kmol · m^{-3} PZ solution at 323 K as a function of CO_2 loading α_{CO_2}.

α_{CO_2}	p_{CO_2}/kPa	pH	Cond./mS	α_{CO_2}	p_{CO_2}/kPa	pH	Cond./mS
0.0633		10.00	3.8	0.418	19.7	9.01	15.8
0.127	0.68	9.66	6.25	0.483	32.8	8.91	18.6
0.155	1.05	9.52	7.0	0.541	45.8	8.77	19.8
0.190	2.00	9.52	8.3	0.584	60.3	8.72	21.8
0.233	3.19	9.30	9.6	0.610	69.5	8.65	22.0
0.255	4.68	9.33	10.4	0.636	84.0	8.62	23.2
0.310	6.99	9.15	12.1	0.657	94.5	8.55	23.4
0.323	8.37	9.15	12.1				

TABLE 10
Experimental equilibrium data (CO_2 partial pressure p_{CO_2}, pH, and conductivity) in a 0.5 kmol · m^{-3} MDEA and 1.5 kmol · m^{-3} PZ solution at 298 K as a function of CO_2 loading α_{CO_2}.

α_{CO_2}	p_{CO_2}/kPa	pH	Cond./mS	α_{CO_2}	p_{CO_2}/kPa	pH	Cond./mS
0.112		11.28	4.5	0.843	10.6	8.35	13.6
0.177		11.12	5.9	0.906	26.8	8.02	14.5
0.278		10.80	8.5	0.909	29.1	7.98	15.0
0.328		10.67	9.1	0.943	53.7	7.75	15.1
0.436		10.32	10.9	0.965	81.1	7.58	15.45
0.502	0.25	10.12	11.5	0.967	80.1	7.58	15.5
0.640	1.02	9.68	12.9	0.978	102	7.47	15.75
0.675	1.55	9.57	12.8	0.984	110	7.44	15.9
0.807	7.15	9.02	13.9				
0.826	9.02	8.98	14.0				

TABLE 11
Experimental equilibrium data (CO_2 partial pressure p_{CO_2}, pH, and conductivity) in a 0.5 kmol · m^{-3} MDEA and 1.5 kmol · m^{-3} PZ solution at 313 K as a function of CO_2 loading α_{CO_2}.

α_{CO_2}	p_{CO_2}/kPa	pH	Cond./mS	α_{CO_2}	p_{CO_2}/kPa	pH	Cond./mS
				0.731	8.1	8.60	19.5
0.0948		10.3	6.2	0.749	9.7	8.55	19.6
0.184		10.04	9.25	0.817	20.1	8.29	20.3
0.281		9.76	12.4	0.865	36.9	8.05	21.0
0.369		9.54	14.1	0.870	38.8	8.07	21.0
0.465	0.45	9.24	17.0	0.900	59.2	7.91	21.4
0.555	1.38	8.97	18.0	0.906	64.1	7.86	21.5
0.649	3.76	8.65	19.6	0.921	79.8	7.79	21.8
0.74	9.24	8.34	20.0	0.923	80.8	7.75	21.5
0.843		7.96	21.0	0.934	96.0	7.88	22.0
				0.936	98.8	7.70	21.9

Additional to the VLE data listed in tables 7 to 11, also the pH values of the lean solutions were determined. For accuracy reasons, these measurements were performed in a separate setup, described by Hamborg *et al.* [39], using a pH glass electrode (Metrohm, type 6.0258.010) with a resolution of 0.1 mV and 0.1 K. The results are listed in table 12.

Parts of the data series in tables 7 to 9 can be compared to data from literature as these data points were measured at similar concentrations and temperatures.

The data listed in table 7 are graphically compared to the equilibrium data reported by Bishnoi and Rochelle [3] in figure 9, and it is obvious from this figure, that both data series are in very good agreement with each other. Moreover, at low loadings a double logarithmic plot shows a linear relation between the CO_2 partial pressure and the equilibrium loading, which proves that the data from the present study are internally consistent (see, *e.g.* [9]).

The (graphical) comparison – shown in figures 10 and 11 – between the experimental CO_2 solubilities in aqueous solutions containing 2.8 kmol · m^{-3} MDEA and 0.7 kmol · m^{-3} piperazine as listed in tables 8 and 9 and the data reported by Liu *et al.* [2], shows the following trends:

- The present experimental data are found to be internally consistent (linear relation in figure 11).
- The new data at 50 °C are well in line with the data reported by Liu *et al.* [2].
- At 30 °C the agreement between both sets of equilibrium data is less satisfactory. Unfortunately, no explanation could be given for this observation.

4.2. NMR speciation results

The NMR spectroscopy data taken in 4.0 kmol · m^{-3} aqueous MDEA activated with 1.0 kmol · m^{-3} piperazine at 298.15 K were analyzed for the concentration of the different piperazine reaction product ratios as explained in the experimental section. The results are listed in table 13.

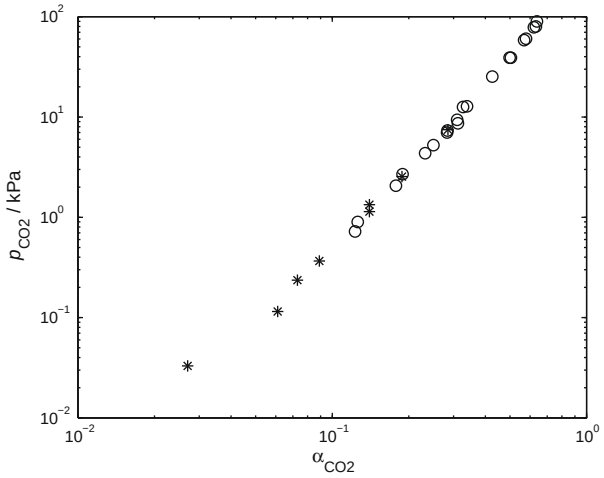

FIGURE 9. CO_2 partial pressure p_{CO_2} as a function of loading α_{CO_2} in 4.0 kmol · m^{-3} MDEA and 0.6 kmol · m^{-3} PZ solution at 313 K: ○, this work; ∗, Bishnoi and Rochelle [3].

TABLE 12
Experimental pH data of the lean aqueous PZ/MDEA solutions.

c_{MDEA} = 4.0 kmol · m^{-3}, c_{PZ} = 0.6 kmol · m^{-3}		c_{MDEA} = 2.8 kmol · m^{-3}, c_{PZ} = 0.7 kmol · m^{-3}		c_{MDEA} = 0.5 kmol · m^{-3}, c_{PZ} = 1.5 kmol · m^{-3}	
T/°C	pH	T/°C	pH	T/°C	pH
24.9	12.09	24.9	12.04	24.9	12.18
29.8	11.96	29.9	11.92	29.9	12.04
40.1	11.71	40.1	11.67	40.1	11.77
50.0	11.45	50.1	11.42	50.2	11.51

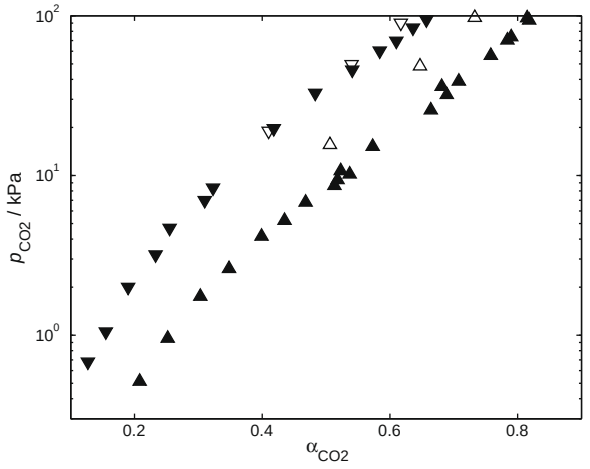

FIGURE 10. CO_2 partial pressure p_{CO_2} as a function of α_{CO_2} in 2.8 kmol · m $^{-3}$ MDEA and 0.7 kmol · m^{-3} PZ solution. At 303 K: ▲, this work; △, Liu *et al.* [2]. At 323 K: ▼, this work; ▽, Liu *et al.* [2].

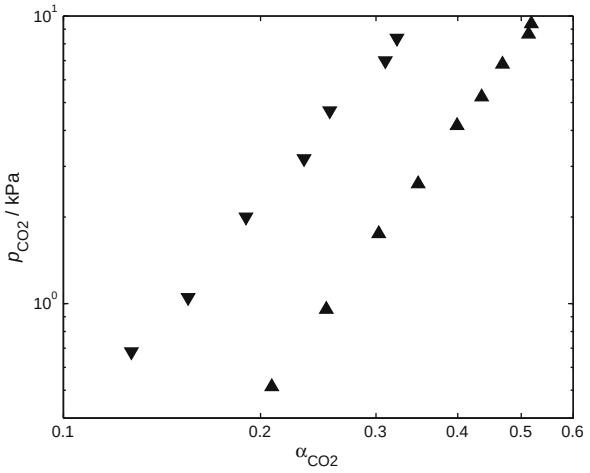

FIGURE 11. CO_2 partial pressure p_{CO_2} as a function of α_{CO_2} in 2.8 kmol · m^{-3} MDEA and 0.7 kmol · m^{-3} PZ solution at low CO_2 loadings. At 303 K: ▲, this work. At 323 K: ▼, this work.

5. Modelling results and discussion

As pointed out earlier in this work, the final thermodynamic model still contains a total of six, at this point unknown, parameters. These latter parameters firstly include the mutual ionic interaction between piperazine and MDEA species. It is clear that these cannot be determined from any other (reactive) subsystem. Secondly, also the binary interaction between PZ and MDEA remains unknown, since in literature no (useful) experimental VLE data on this subsystem are available. Overall, a total of six adjustable parameters will be regressed over a selection of experimental pressure data reported on the aqueous (CO_2 + PZ + MDEA) system.

As already mentioned in Section 1, several experimental VLE data series are available in the literature. These data series were divided into three categories with respect to the regression of the remaining adjustable parameters:

1. A regression set: This selection of experimental data will be used in the actual regression of the adjustable parameters;
2. An extrapolation set: The VLE data in this set will be compared to model predictions obtained using the model and the adjustable parameters as obtained in the regression with the regression set;
3. Non-reliable experimental data: These data will not be used in the regression nor the extrapolation part of the simulation.

Figure 2 on the solubility of CO_2 in aqueous 2.0 kmol · m^{-3} MDEA illustrates that the equilibrium partial pressures reported by Si Ali and Aroua [5] are considerably lower than the other literature sources, especially at lower carbon dioxide loadings, and hence their data might be prone to experimental error. As this also raises questions concerning the reliability of their solubility data in aqueous MDEA/PZ solutions, the data of Si Ali and Aroua [5] were classified as aforementioned category 3 data.

A detailed description of both the regression set (category 1) and the extrapolation set (category 2) data is given below.

The experimental database used in the regression (category 1) contained the experimental data series reported by Bishnoi and Rochelle [3], Liu *et al.* [2], Pérez-Salado Kamps *et al.* [4], thereby including solubility data taken at a wide range of experimental conditions (see table 14). The following remarks should be made regarding the final regression:

- The data series reported by Liu *et al.* [2] on solubilities in solutions containing 4.77 kmol · m^{-3} MDEA and 0.53 kmol · m^{-3} PZ were excluded from the regression, as the MDEA concentration exceeded the maximum concentration (4.3 kmol · m^{-3}) taken into consideration in the MDEA ternary subsystem which has been discussed earlier. These particular data, however, have been added to the extrapolation data set (category 2);
- Also, preliminary model optimization runs were conducted and data points for which the difference between experimentally determined and model predicted (CO_2 partial and/or total) pressure was more than a factor two, were also eliminated from the database;
- These preliminary model optimization runs also indicated that the model showed little to no sensitivity to the (adjustable) parameters describing the interaction between $MDEAH^+$ and

TABLE 13
Liquid phase speciation of a 4.0 kmol · m^{-3} MDEA, 1.0 kmol · m^{-3} PZ at 298.15 K as determined by NMR.

Sample/run[b]	α_{CO_2}	PZ: MDEA[a]	$C_{PZ} + C_{PZH^+}$/(kmol · m^{-3})	$C_{PZCOO^-} + C_{^+HPZCOO^-}$/(kmol · m^{-3})	$C_{PZ(COO^-)_2}$/(kmol · m^{-3})
2	0.070	0.24	0.67	0.30	0.029
3a	0.100	0.24	0.58	0.37	0.055
3b	0.100	0.24	0.57	0.37	0.056
4a	0.053	0.24	0.77	0.22	0.013
4b	0.053	0.24	0.76	0.23	0.014
5	0.108	0.24	0.51	0.41	0.079
6[c]	0.210	0.24	0.52	0.40	0.078

[a] Ratio between total PZ species and total MDEA species.
[b] Runs a and b are duplicate experiments taken with the same sample.
[c] Sample 6 was prepared by adding extra carbon dioxide to sample 5.

TABLE 14
Experimental database used in regression of quaternary (ionic) interaction parameters.

	$c_{MDEA}/(kmol \cdot m^{-3})$	$c_{PZ}/(kmol \cdot m^{-3})$	T/K	α_{CO_2}	N/n^a	AAD/%
[3]	4.0	0.6	313	0.027 to 0.285	8/8	31.1
	4.0	0.6	343	0.014 to 0.093	3/5	27.7
[2]	1.35	0.35	323; 343	0.349 to 0.955	10/10	18.9
	1.53	0.17	323; 343	0.387 to 0.980	10/10	18.7
	2.8	0.7	303; 323; 343; 363	0.147 to 0.842	14/20	23.4
	3.15	0.35	303; 323; 343; 363	0.198 to 0.880	15/20	25.5
	3.75	1.55	323; 343	0.247 to 0.746	10/10	34.4
[4]	2.0 mol · kg^{-1}	2.0 mol · kg^{-1}	353	0.64 to 1.13	10/10	6.5
Total					80/93	22.8

[a] Experimental data points used/ Total reported experimental data points.

$PZCOO^-$ and the interaction between PZH^+ and MDEA. Therefore, these parameters were set to an arbitrary value of 0.010 kmol · m^{-3} (see also table 15). It should be noted, that the negligible sensitivity of the model towards these parameters might just be a "local" effect and this might thus change when the values of the other four interaction parameters are changed considerably;

- Finally, during the preliminary runs it was observed that model calculations for low loading data showed a large sensitivity towards the binary parameter k_{mix} describing the interaction between piperazine and MDEA. The effect of the regressed ionic parameters was more pronounced at moderate to high carbon dioxide loading cases.

The final experimental database used in the regression of the parameters is specified in detail in table 14. Results of the model optimization are listed both in table 15 (regressed parameter values) and table 14 (average deviations between experiment and model) and a parity plot between experimental value and model description is given in figure 12.

From table 14 and figure 12, it can be concluded that the present model is able to correlate experimental (total and CO_2 partial) pressure data within an average absolute deviation of about 23% over all the experimental conditions included in the experimental database in table 14.

Next, the model's extrapolation qualities were explored using the experimental data series that were not used in the parameter regression: These data not only include the experimental VLE data measured in the present study, but also the experimental solubilities reported by Xu *et al.* [1] and the one series from the experimental data of Liu *et al.* [2] which was left out of regression set. A comparison between the experimentally obtained and model predicted values is given graphically in figure 13.

From the results shown in figure 13 and table 16, the following can be concluded with respect to the different data sets:

- Model predicted CO_2 partial pressures are in good agreement with the experimental data reported by Xu *et al.* [1];

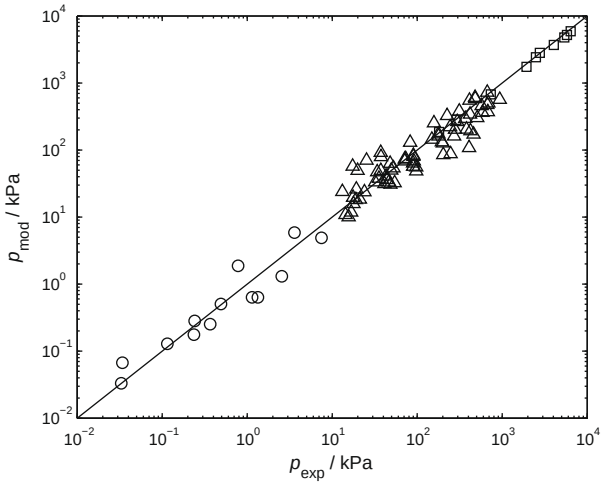

FIGURE 12. Parity plot of experimentally determined equilibrium pressures p_{exp} and modelling results p_{mod}: ○, Bishnoi and Rochelle [3]; △, Liu *et al.* [2]; □, Pérez-Salado Kamps *et al.* [4].

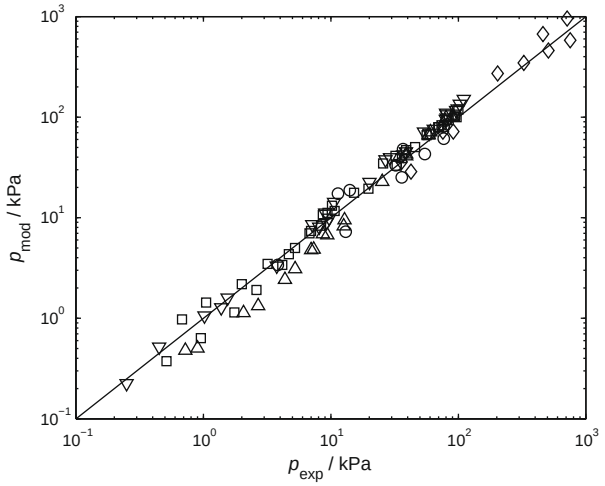

FIGURE 13. Parity plot of experimentally determined equilibrium pressures p_{exp} and modelling results p_{mod}: ○, Xu *et al.* [1]; ◇, Liu *et al.* [2]; △, this work in '4.0 MDEA/0.6 PZ'; □, this work in '2.8 MDEA/0.7 PZ'; ▽, this work in '0.5 MDEA/1.5 PZ'.

TABLE 15
Resulting values of the regressed interaction parameters.

Parameter-type	Species	Final value[a]
k_{mix}	MDEA–PZ	−0.46
W	$MDEAH^+$–PZ	0.425 m^3 · kmol $^{-1}$
W	$MDEAH^+$—$^+HPZCOO^-$	0.100 m^3 · kmol^{-1}
W	$MDEAH^+$–$PZCOO^-$	0.010 m^3 · kmol^{-1}
W	$MDEAH^+$—$PZ(COO^-)_2$	−0.555 m^3 · kmol^{-1}
W	PZH^+–MDEA	0.010 m^3 · kmol^{-1}

[a] The ionic interaction parameters between $MDEAH^+$ and $PZCOO^-$, and PZH^+ and MDEA were not regressed, as discussed earlier.

- The model is well able to predict the experimental solubility data of Liu *et al.* [2] in aqueous 4.77 kmol · m^{-3} MDEA/ 0.53 kmol · m^{-3} PZ solutions, which were left out of the parameter regression;
- All three presently reported new experimental data series are predicted well by the model.

TABLE 16
Experimental solubility data that were not used in the regression.

	$c_{MDEA}/(kmol \cdot m^{-3})$	$c_{PZ}/(kmol \cdot m^{-3})$	T/K	α_{CO_2}	N	AAD
[1]	4.28	0.103; 0.257; 0.515	343	0.052 to 0.29	11	23.5
[2]	4.77	0.53	323, 343	0.193 to 0.760	10	21.0
This work	4.0	0.6	313	0.123 to 0.638	20	27.2
	2.8	0.7	303, 323	0.127 to 0.837	36	16.2
	0.5	1.5	298, 313	0.465 to 0.984	28	19.6

Other experimental data to validate the model are (direct and/or indirect) speciation data, such as pH, conductivity, and NMR data. Figures 14 and 15 show a comparison between model predicted pH and conductivity (as the total ion mole fraction present in the liquid) in an aqueous 4.0 $kmol \cdot m^{-3}$ MDEA/0.6 $kmol \cdot m^{-3}$ PZ solution at 313 K, and the presently obtained experimental data listed in table 7.

Figure 14 illustrates – as in the case for the aqueous MDEA solution shown earlier (figure 8) – that, although the model is able to describe the experimentally observed trend in pH with increasing loading, it cannot predict the absolute pH values accurately. Figure 15 shows that the total ion mole fractions predicted by the model are in line with the experimentally observed trend in conductivity. Similar plots and trends are found when comparing model predictions to the other experimental pH and conductivity data listed in tables 8 to 11.

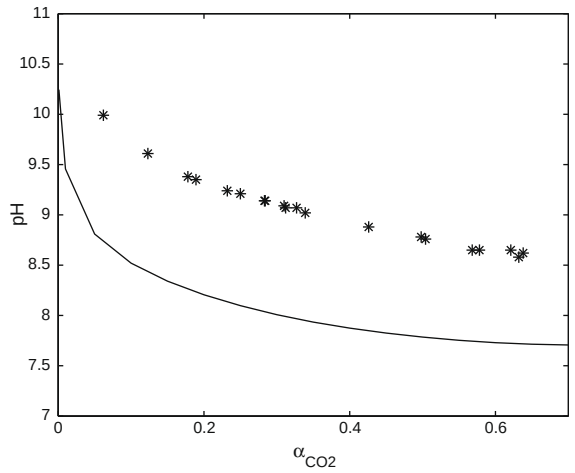

FIGURE 14. pH of an aqueous 4.0 $kmol \cdot m^{-3}$ MDEA/0.6 $kmol \cdot m^{-3}$ PZ solution at 313 K as a function of CO_2 loading α_{CO_2}: ∗, experiment – this work; 'solid line', model prediction.

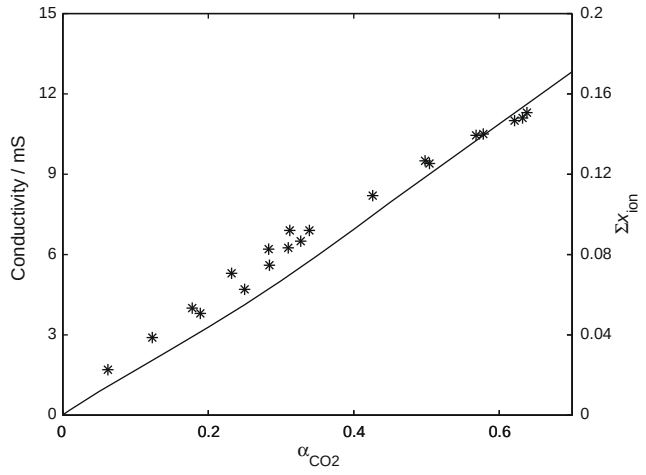

FIGURE 15. Conductivity of an aqueous 4.0 $kmol \cdot m^{-3}$ MDEA/0.6 $kmol \cdot m^{-3}$ PZ solution at 313 K as a function of CO_2 loading α_{CO_2}: ∗, experiment – this work; 'solid line', model prediction.

The experimentally determined pH data of lean solutions, listed in table 12, serve as the basis of a second comparison between model prediction and experimental value. In table 17, these experimental data – as well as the experimental pH of a 50 wt.% MDEA solution – are compared to predictions made with the EoS model. Table 17 also contains the pH as calculated when assuming the solution behaves ideally (*i.e.* $\gamma = 1$). Again, the comparison shows that an offset exists between experimental and model predicted pH value.

A comparison between the model predicted liquid phase composition and the available experimental NMR speciation data [3] are given in table 18 and figure 16 (present data, see also table 13).

The generally observed trend as seen in figure 16 seems logical – at least for loadings up to about 0.12:

- With increasing loading, the relative amount of (protonated) piperazine (Fraction I) decreases;
- With increasing loading, the relative amount of (protonated) piperazine carbamate (Fraction II) increases;
- With increasing loading, the relative amount of piperazine dicarbamate (Fraction III) increases.

However, the speciation at a loading of 0.21 seems to deviate from the aforementioned trend. The speciation seems nearly identical to that at a loading of 0.108, but at this moment no explanation can be presented for this observation.

Figure 16 shows that the model seems to predict the experimentally observed trends in speciation data qualitatively well over the range studied. However, both figure 16 and table 18 illustrate that the model, *e.g.* tends to overpredict the amount of dicarbamated piperazine, whereas the fraction of the monocarbamate species is underpredicted.

Based on the results obtained in both the prediction of the solubility – (partial) pressure data (table 16, figure 13) and the speciation study (table 18, figure 16), it should be concluded that although the model is generally well suited to describe and predict the so-called "$p - \alpha$" data, the model in its current form seems not to be able to predict the speciation in the quaternary system $PZ + MDEA + CO_2 + H_2O$ satisfactorily over all experimental conditions studied.

However, based on the results obtained so far, the Electrolyte EoS model does show very promising results. Firstly, it should be stressed that in the EoS approach, it is possible to build a multiple component system from smaller, 'lower level' systems – as, *e.g.* illustrated in figure 3 – without the need for adjusting parameters when going from one level to a higher level. The direct consequence (and a major advantage) is that the amount of adjustable parameters per (sub)system is limited. Secondly, it should be noted that various additional improvements can be made to the model in its current state to the determination of the required interaction parameters – especially in some of the lower level subsystems,

TABLE 17
Model predicted and experimental pH values of lean solutions.

Solution	T/°C	pH_{exp}	pH_{ideal}	pH_{EoS}[a]	pH_{EoS}[b]
50 wt.% MDEA[c]	23.3	11.72	11.77	11.03	
$c_{MDEA} = 4.0$ kmol · m^{-3}, $c_{PZ} = 0.6$ kmol · m^{-3}	25.0	12.09	11.98	10.91	10.93
	30.0	11.96	11.84	10.75	10.77
	40.0	11.71	11.58	10.46	10.48
	50.0	11.45	11.34	10.20	10.22
$c_{MDEA} = 2.8$ kmol · m^{-3}, $c_{PZ} = 0.7$ kmol · m^{-3}	25.0	12.04	11.94	10.95	10.97
	30.0	11.92	11.80	10.80	10.82
	40.0	11.67	11.53	10.53	10.55
	50.0	11.42	11.29	10.28	10.30
$c_{MDEA} = 0.5$ kmol · m^{-3}, $c_{PZ} = 1.5$ kmol · m^{-3}	25.0	12.18	12.00	11.66	11.66
	30.0	12.04	11.86	11.50	11.50
	40.0	11.77	11.59	11.20	11.20
	50.0	11.51	11.34	10.92	10.93

[a] Calculated at a CO_2 loading of 10^{-4}.
[b] Calculated at a CO_2 loading of 10^{-5}.
[c] Taken from Posey [33], CO_2 loading = 10^{-4}.

TABLE 18
Experimental and model predicted speciation in 3.0 kmol · m^{-3} MDEA/1.0 kmol · m^{-3} PZ solution with a CO_2 loading of 0.52 at 298 K.

Piperazine species	Fraction of total piperazine	
	Experiment[a]	Model
PZ + PZH^+	0.13	0.08
$PZCOO^-$ + $^+HPZCOO^-$	0.53	0.22
$PZ(COO^-)_2$	0.34	0.70

[a] Calculated from ratios given by Bishnoi and Rochelle [3].

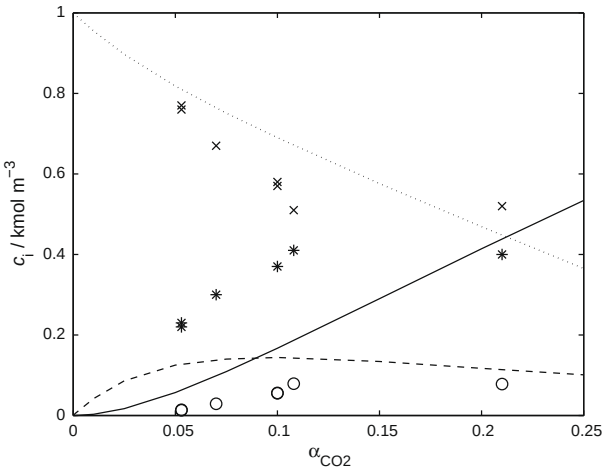

FIGURE 16. Liquid phase speciation in concentration c_i of an aqueous 4.0 kmol · m^{-3} MDEA/1.0 kmol · m^{-3} PZ solution loaded with CO_2 at 298 K as as a function of CO_2 loading α_{CO_2}. Fraction I: ×, experiment; 'dotted line', model. Fraction II: ∗, experiment; 'dashed line', model. Fraction III: ○, experiment; 'solid line', model.

where educated guesses were necessary to determine several interaction parameters.

The first improvements can be made with regard to the binary interaction parameters involving MDEA, PZ, and H_2O which are to be regressed on experimental VLE data on the respective physical systems. And, while few experimental data have been reported on the (MDEA + H_2O) system, no (useful) data are available on the system (PZ + H_2O) and (MDEA + PZ). At present, the required binary interaction between piperazine and water has been estimated using pseudo data generated with the UNIFAC method [11], while the MDEA–PZ interaction has been included using a single mixing parameter, which was regressed together with the quaternary ionic interaction parameters. It is known in the literature, that acid gas solubility models exhibit a high sensitivity towards the amine–water interaction, especially at low loadings (see, *e.g.* [21]). Based on the modelling results obtained in this work it can be said that the same conclusion holds for the interaction between piperazine and MDEA. The same can be concluded from the modelling work done by Bishnoi and Rochelle [3], who reported that a precise fit of their (low loading) solubility data could only be obtained, when the binary PZ–MDEA interaction parameters present in their Electrolyte NRTL model were regressed. This implies, that experimental VLE data on these systems are vital for a more accurate determination of the corresponding interaction parameters.

Secondly, in the EoS studies carried out so far and including this one, the $p - \alpha$ data of ternary and quaternary systems have been taken as the single (and only) source for the regression of interaction parameters. Based on the results seen in this study, it is suggested to also include other types of experimental data in the optimization of the interaction parameters, such as NMR speciation data, conductivity data and pH data. Including other data than the conventional VLE data in the regression of interaction parameters should be done at the lowest possible level (see figure 3), so that the basis of the determination of the interaction parameters to be used in higher order systems becomes much more solid and thus reduce the uncertainty in these parameters considerably. Problem in this might be the formulation of a good target function for minimization, in which an appropriate weight is attributed to the various experimental results (*i.e.* $p - \alpha$ data, speciation data, pH, conductivity).

All these efforts will help to make that the Electrolyte EoS model cannot only satisfactorily describe and predict the carbon dioxide partial pressure over a loaded solution, but also correctly predict speciation data. This way it will become a very powerful tool in rate based (rigorous) modelling of industrial absorber and desorber columns.

6. Conclusions

The bulk removal of carbon dioxide from process gas streams is, in industry, usually carried out via an absorber–desorber process operation. One promising solvent used in this process step is the piperazine (PZ) activated aqueous N-methyldiethanolamine (MDEA) solution, since it combines the benefits of both PZ (high rate of reaction with CO_2) and MDEA (a low reaction enthalpy with

CO_2). An accurate design and modelling of the absorption–desorption process requires detailed knowledge concerning the thermodynamics of these absorbent systems, not only to calculate carbon dioxide partial pressures at specific experimental conditions, but also to predict the liquid phase composition, which is an essential input in rate based column models. In the present study, new experimental CO_2 solubility data in aqueous solutions containing both MDEA and PZ are reported, which not only list the carbon dioxide partial pressure at a certain CO_2 liquid loading, but also the corresponding conductivity and pH of the solution. In addition to these data, NMR spectroscopy has been applied to obtain experimental data on the liquid phase speciation of an aqueous MDEA–PZ solution, partially loaded with carbon dioxide.

Simultaneously, the Electrolyte Equation of State (EoS) model, which was used in previous work to successfully describe the thermodynamics of the (piperazine + water + carbon dioxide) system, was extended to include MDEA. Prior to the extension, the ternary subsystem ($MDEA + H_2O + CO_2$) needed to be described in order to obtain information concerning the interaction parameters unique to this system. It was found, that the Electrolyte EoS model was able to describe the available $p - \alpha$ data reasonably well, and moreover, also the model predicted liquid phase speciation was well in line with the experimental composition data reported by Poplsteinova Jakobsen *et al.* [17].

On application of the total model to the quaternary ($PZ + MDEA + CO_2 + H_2O$) system, it was observed that a total of four adjustable parameters needed to be regressed on experimental solubility data. The final model derived was found to correlate a wide selection of experimental solubility data well, and furthermore the model was able to predict the new experimental $p - \alpha$ data as obtained in this study. The model calculated liquid phase composition, however, did not match the limited available experimental (NMR) data, and therefore it should be concluded that the model in its current state is still not optimally suited for application in rigorous mass transfer models.

Nevertheless, the Electrolyte EoS model has shown very promising results, which is remarkable when considering the relatively high uncertainties in the current binary parameters describing the binary systems involving piperazine and/or MDEA (such as PZ—H_2O and PZ–MDEA). Hence, more experimental VLE data on these physical subsystems are essential for a further development and refinement of the Electrolyte Equation of State. Moreover, the need for additional liquid phase speciation data should be stressed, as the strength of a thermodynamic model is, in the end, truly determined by its ability to predict speciation in a reliable and realistic manner.

Acknowledgements

The authors wish to acknowledge H.F.G. Moed for the construction of the experimental setups, and C. van Aken, E.S. Hamborg, A.R. Hansmeier, and T. Kolkman for their respective contributions to the experimental work. Furthermore, A.H. Velders is acknowledged for the NMR spectroscopy experiments. Shell Global Solutions Nederland BV is acknowledged for their financial support. This research is part of the CATO programme, the Dutch national research programme on CO2 Capture and Storage. CATO is financially supported by the Dutch Ministry of Economic Affairs (EZ) and the consortium partners (http://www.co2-cato.nl).

References

[1] G.-W. Xu, C.-F. Zhang, A.-J. Qin, W.-H. Gao, H.-B. Liu, Ind. Eng. Chem. Res. 37 (1998) 1473–1477.
[2] H.-B. Liu, C.-F. Zhang, G.-W. Xu, Ind. Eng. Chem. Res. 38 (1999) 4032–4036.
[3] S. Bishnoi, G.T. Rochelle, Ind. Eng. Chem. Res. 41 (2002) 604–612.
[4] Á. Pérez-Salado Kamps, J. Xia, G. Maurer, AICHE J. 49 (2003) 2662–2670.
[5] B. Si Ali, M.K. Aroua, Int. J. Thermophys. 25 (2004) 1863–1870.
[6] W. Fürst, H. Renon, AICHE J. 39 (1993) 335–343.
[7] H. Planche, W. Fürst, Entropie 202/203 (1997) 31–35.
[8] G. Vallée, P. Mougin, S. Jullian, W. Fürst, Ind. Eng. Chem. Res. 38 (1999) 3473–3480.
[9] L. Chunxi, W. Fürst, Chem. Eng. Sci. 55 (2000) 2975–2988.
[10] E. Solbraa, Ph.D. Thesis, Norwegian University of Science and Technology, 2002.
[11] P.W.J. Derks, H.B.S. Dijkstra, J.A. Hogendoorn, G.F. Versteeg, AICHE J. 51 (2005) 2311–2327.
[12] D.M. Austgen, G.T. Rochelle, Ind. Eng. Chem. Res. 30 (1991) 543–555.
[13] R.J. Mac Gregor, A.E. Mather, Can. J. Chem. Eng. 69 (1991) 1357–1366.
[14] S.H. Huang, H.J. Ng, GPA Res. Rep. 155 (1998) 8.
[15] S. Bishnoi, G.T. Rochelle, Chem. Eng. Sci. 55 (2000) 5531–5543.
[16] V. Ermatchkov, Á. Pérez-Salado Kamps, G. Maurer, J. Chem. Therm. 35 (2002) 1277–1289.
[17] J. Poplsteinova Jakobsen, J. Krane, H.F. Svendsen, Ind. Eng. Chem. Res. 44 (2005) 9894–9903.
[18] T.E. Daubert, G. Hutchison, AICHE Symp. Series 86 (1990) 93–114.
[19] O. Noll, A. Valtz, D. Richon, T. Getachew-Sawaya, I. Mokbel, J. Jose, Int. Elec. J. Phys. Chem. Data 4 (1998) 105–119.
[20] D.M. Von Niederhausern, G.M. Wilson, N.F. Giles, J. Chem. Eng. Data 51 (2006) 1985–1990.
[21] H.-T. Chang, M. Posey, G.T. Rochelle, Ind. Eng. Chem. Res. 32 (1993) 2324–2335.
[22] E. Voutsas, A. Vrachnos, K. Magoulasm, Fluid Phase Equilib. 224 (2004) 193–197.
[23] S. Xu, S. Qing, Z. Zhen, C. Zhang, J.J. Carroll, Fluid Phase Equilib. 67 (1991) 197–201.
[24] A. Barreau, P. Mougin, C. Lefebvre, Q.M. Luu Thi, J. Rieu, J. Chem. Eng. Data 52 (2007) 769–773.
[25] P.J.G. Huttenhuis, N.J. Agrawal, E. Solbraa, G.F. Versteeg, Fluid Phase Equilib. 264 (2008) 99–108.
[26] G.F. Versteeg, W.P.M. Van Swaaij, J. Chem. Eng. Data 33 (1988) 29–34.
[27] H. Kierzkowska-Pawlak, R. Zarzycki, J. Chem. Eng. Data 47 (2002) 1506–1509.
[28] Y.W. Wang, S. Xu, F.D. Otto, A.E. Mather, Chem. Eng. J. 48 (1992) 31–40.
[29] A. Jamal, Ph.D. Thesis, University of British Columbia, 2002.
[30] P.J.G. Huttenhuis, N.J. Agrawal, J.A. Hogendoorn, G.F. Versteeg, J. Petr. Sci. Eng. 55 (2007) 122–134.
[31] M.L. Posey, G.T. Rochelle, Ind. Eng. Chem. Res. 36 (1997) 3944–3953.
[32] Á. Pérez-Salado Kamps, G. Maurer, Chem. Eng. Data 41 (1996) 1505–1513.
[33] M.L. Posey, Ph.D. Thesis, University of Texas, 1996.
[34] B. Lemoine, Y.-G. Li, R. Cadours, C. Bouallou, D. Richon, Fluid Phase Equilib. 172 (2000) 261–277.
[35] G. Kuranov, N. Rumpf, G. Maurer, N. Smirnova, Fluid Phase Equilib. 136 (1997) 147–162.
[36] S.W. Rho, K.P. Yoo, J.S. Lee, S.C. Nam, J.E. Son, B.M. Min, J. Chem. Eng. Data 42 (1997) 1161–1164.
[37] Á. Pérez-Salado Kamps, A. Balaban, M. Jödecke, G. Kuranov, N.A. Smirnova, G. Maurer, Ind. Eng. Chem. Res. 40 (2001) 696–706.
[38] W.J. Rogers, J.A. Bullin, R.R. Davidson, AICHE J. 44 (1998) 2423–2430.
[39] E.S Hamborg, J.P.M Niederer, G.F. Versteeg, in: Proceedings of the 8th International Conference on Greenhouse Gas Control Technologies (GHGT-8) in Trondheim, Norway, 2006.

JCT 08-422